International Journal of Mineral Processing and Extractive Metallurgy
2022; 7(3): 75-84
http://www.sciencepublishinggroup.com/j/ijmpem
doi: 10.11648/j.ijmpem.20220703.12
ISSN: 2575-1840 (Print); ISSN: 2575-1859 (Online)

Interfacial Microstructure Evolution and Mechanical Properties of Laser Welding Joints for Stainless Steel to TiNi Shape Memory Alloy

Zhijin Guo[1], Yan Zhang[1, *], Jianping Zhou[1], Daqian Sun[2], Hongmei Li[2]

[1]School of Mechanical Engineering, Xinjiang University, Urumchi, China

[2]Key Laboratory of Automobile Materials, School of Materials Science and Engineering, Jilin University, Changchun, China

Email address:

yanzhang4967@163.com (Yan Zhang)

[*]Corresponding author

To cite this article:

Zhijin Guo, Yan Zhang, Jianping Zhou, Daqian Sun, Hongmei Li. Interfacial Microstructure Evolution and Mechanical Properties of Laser Welding Joints for Stainless Steel to TiNi Shape Memory Alloy. *International Journal of Mineral Processing and Extractive Metallurgy*. Vol. 7, No. 3, 2022, pp. 75-84. doi: 10.11648/j.ijmpem.20220703.12

Received: April 17, 2022; **Accepted**: June 24, 2022; **Published**: July 20, 2022

Abstract: In this paper, laser welding of stainless steel and TiNi shape memory alloy dissimilar materials was carried. Microstructures of the joints were analyzed by means of scanning electron microscopy (SEM), energy dispersive spectroscopy (EDS) and X-ray diffraction (XRD). Mechanical properties of the joints were evaluated by tensile tests. Based on avoiding the formation of Ti-Fe intermetallics in the joint, three welding processes for SS-TiNi alloy joint were introduced. The joint A was formed while the laser was acted on the SS-TiNi alloy interface and joint fractured along the SS side in weld immediately after welding without filler metal. The joint B was formed while the laser was acted on the Cu interlayer. Experimental results showed that Cu interlayer was helping to decrease the Ti-Fe intermetallics by forming Ti-Cu phases in the weld. The tensile strength of the joint B was 216 MPa. The joint C was formed while the laser was acted on the SS side 1.0 mm. One process was one pass welding involving creation of a joint with one fusion weld and one brazed weld separated by remaining unmelted SS. The mechanical performance of the joint C was determined by the brazed weld formed at SS-TiNi alloy interface with a tensile strength of 256 MPa.

Keywords: Stainless Steel, TiNi Alloy, Cu Interlayer, Laser Welding, Microstructure, Tensile Strength

1. Introduction

TiNi shape memory alloys is one kind of new functionality material. It has special shape memory effect and superelasticity, excellent anti-erosion ability and great biocompatibility. It has broad application prospects in aerospace, atomic energy, marine development, mechatronics and medical equipment [1-3]. As we all know, every the successful application of advanced material depends not only on itself inherent properties, but also on the development of technology that the connection of TiNi alloy with itself or other materials [4-5]. At present, the successful welding of TiNi alloys, especially laser welding, has been well confirmed. As heterogeneous joints play a considerable role in reducing raw material costs and improving design conditions, the demand for such joints has accelerated over the past two decades [6-7]. However, there are few research on welding TiNi alloys with other materials, such as stainless steel (SS). Because of stainless steel excellent mechanical properties, low cost, and corrosion resistance, it has been widely used to medical devices [8-9]. In many applications, the combination of TiNi alloy and stainless steel will be an ideal material combination. However, the huge differences in physical and chemical properties of these two materials made the welding of dissimilar materials complicated and difficult. The formation of Ti-Fe intermetallic compounds during welding are the main factors that reduce the mechanical properties of joints [10]. The formation of these Ti-Fe intermetallic compounds in the weld metal made brittle. The combination of the formation of this brittle Ti-Fe intermetallic compounds and the complex residual stresses formed in the weld due to the mismatch of the thermal expansion coefficients of the two materials leads to the formation of cracks in the weld,

thereby limiting the application of heterogeneous joints in many industries [11-12]. In fact, increasing the use of lightweight materials such as TiNi alloys and adopting lightweight structures in the aerospace and engineering manufacturing fields is one of the most direct and effective ways to achieve structural optimization, energy saving, environmental protection and safety [13]. The effective connection between the TiNi alloy and SS heterogeneous material has become an urgent problem.

At present, it is possible to increase the solidification rate of the weld by adding an interlayer to change the chemical composition of the weld, and using a highly thermally conductive substrate as a heat sink, which is one of the solutions to limit the formation of Ti-Fe intermetallic compounds in the weld [14-15]. Another way to limit the formation of Ti-Fe intermetallic compounds in the weld metal is to adjust welding parameters to minimize heat input to promote higher solidification rates [16]. This is because the lower the heat input, the higher the solidification rate of the weld metal. The increase in the solidification rate limits the formation of Ti-Fe intermetallic compounds, thereby improving the mechanical properties of the joint. Copper is a soft metal and have lower melting point than SS and TiNi alloy. Therefore, it can reduce the effect of thermal stress mismatch caused by solidification of the welding pool during welding [17]. According to the research conducted by Bricknell et al [18], in the Ti-Cu-Ni ternary shape memory alloy, nickel atoms can be replaced with copper atoms in the lattice structure. This substitution led to the formation of Ti (Ni, Cu) ternary alloys at different transition temperatures. Therefore, Cu has good compatibility with TiNi alloys. In addition, Cu neither reacted with Fe nor formed any brittle intermetallic compounds with Fe in the weld metal. Therefore, Cu could be used as an interlayer for welding dissimilar materials of SS and TiNi alloy. A. Shojaei Zoeram reported that the brittle intermetallic phase, $TiFe_2$, made the resulting weld equally brittle and laser welding using Cu interlayer could greatly improve the mechanical performance of TiNi alloy-SS fusion welds [19]. Cu has lower melting point and yield strength as well as good ductility and deformation capacity which would improve fluidity of welding pool and the brittleness of the joints. According to the above analysis, when an interlayer is added during welding, the metallurgical reaction of Ti and Fe in the weld is significantly suppressed, and the content of Ti-Fe intermetallic compounds in the weld is greatly reduced, resulting in a relatively stable welding joint [20]. However, no matter what interlayer is used, as long as the interlayer is completely melted, Ti and Fe elements will be mixed and reacted in the welding pool, and Ti-Fe intermetallic compounds will inevitably be formed in the welding pool. Therefore, the formation of Ti-Fe intermetallic compounds in the weld cannot be avoided only by adding an interlayer [21]. The presence of Ti-Fe intermetallic compounds still has a large impact on the performance of joints. It has been reported that the weld microstructures and joint properties can be improved by using AgCu interlayer in transient liquid phase diffusion bonding (TLP-DB) [22-23], silver based fillers in laser-brazing [24] and brazing [25], and Ni interlayer in friction welding [26]. In the processes mentioned above, the joints are formed without large-scale melting of the base metals (TiNi alloy and SS). Therefore, the absence of liquid mixing of the base metals during welding can minimize or avoid the formation of brittle Ti-Fe intermetallic compounds. However, these welding processes are usually limited to joints of a specific geometry and size. Therefore, the weldability between TiNi alloy and SS dissimilar materials is poor, which seriously deteriorates the performance and connection quality of the joint. This has become one of the key scientific and technological issues that restrict the optimization design and application of the aerospace field, nuclear reaction engineering, and major equipment structures.

Welding metallurgy and weldability of dissimilar materials are the main content of welding theory research and the basis of welding technology research and development. Therefore, the purpose of this research is to carry out basic research on welding metallurgy, weldability, and practicality of TiNi alloy and SS dissimilar materials. This can not only enrich the basic theory of welding of dissimilar materials, but also help promote the development of welding technology, lightweight technology and major equipment manufacturing technology. In this study, the microstructure characterization and mechanical property testing of the laser welded joints of TiNi alloy and SS were carried out in order to explore an ideal welding process to further improve the bonding strength of TiNi alloy and SS. After welding, the appearance, mechanical properties, element orientation, intermetallic compounds, crystallization behavior, and connection mechanism of the weld were evaluated.

2. Experimental Procedure

2.1. Materials

The base materials used in this experiment were TiNi alloy and 304 SS. Their chemical compositions and physical properties are given in Tables 1, 2 and 3. It can be seen that there are large differences in thermal conductivity and linear expansion coefficient between the two base materials, which would lead to large temperature gradient and thermal stress in the joint during welding process. The base materials were machined into 50 mm×40 mm×1 mm plates, and then cleaned with acetone before welding. 0.3 mm thick Cu sheet (99.99 at. %) were adopted as interlayer and placed on the contact surface of the base material fixed in fixture. The filler metal used was 0.2 mm plate of Ag-base filler metal (45 wt.% Ag, 30 wt.% Cu and 25 wt.% Zn).

Table 1. *Main chemical compositions of TiNi alloy (at.%).*

C	Co	Cu	Cr	Nb	Ni	Fe	Ti
0.045	0.005	0.005	0.005	0.005	55.72	0.012	Bal

Table 2. *Main chemical compositions of 304 stainless steel (at.%).*

Si	Mn	P	S	Cr	Ni	N	Fe
0.53	1.07	0.04	0.03	18.09	8.01	0.03	Bal

Table 3. *Physical properties of TiNi alloy and 304 stainless steel.*

Material	Melting point/°C	Tensile strength/MPa	Specific heat capacity / ($J.kg^{-1}.K^{-1}$)	Thermal conductivity / ($W.m^{-1}.K^{-1}$)	Linear expansion coefficient ($10^{-6}.K^{-1}$)
SS	1450	550	500	16.3	16.9
TiNi	1275	800	460	10	10

2.2. Welding Method

Continuous wave laser was used with average power of 1.20 kW, wavelength of 1080 nm and beam spot diameter of 0.1 mm. Schematic diagram of the welding process is shown in Figure 1, where a good fit-up between the TiNi-Cu-SS was required to prevent gaps and ensure adequate heat transfer to form a joint. Welding conditions of three joints are provided below.

Laser welding for joint A. During welding, laser beam was focused on the centerlines of the TiNi-SS interface (Figure 1a). It was important to set up welding parameters to ensure that base materials was completely melted. Laser offset for weld of joint A was defined as 0 mm. The welding process parameters were: laser beam power of 420 W, defocusing distance of + 5 mm, welding speed of 650 mm/min.

Laser welding for joint B. During welding, laser beam was focused on the centerlines of the Cu interlayer (Figure 1b). According to the thickness of the Cu interlayer to adjust welding parameters. At the same time can adjust welding parameters to change the fusion ratio of the base materials. Laser offset for weld of joint B was defined as 0 mm. The welding process parameters were: laser beam power of 432 W, defocusing distance of + 5 mm, welding speed of 650 mm/min.

Laser welding for joint C. In order to ensure that SS was not completely melted, the laser beam was focused on the SS plate 1.0 mm away from the SS-filler metal interface (Figure 1c). The unmelted part of SS acted as a heat sink due to its high thermal conductivity absorbing a significant amount of energy from the welding pool and transferring it to the TiNi side. Laser offset for weld of joint C was defined as 1.0 mm. The welding process parameters were: laser beam power of 432 W, defocusing distance of + 5 mm, welding speed of 650 mm/min.

Argon gas with the purity of 99.99% was applied as a shielding gas with total flow of 20 L/min at top of the joint. Supplementary gas protection device covering the melted zone has been used to minimize the risk of oxidation.

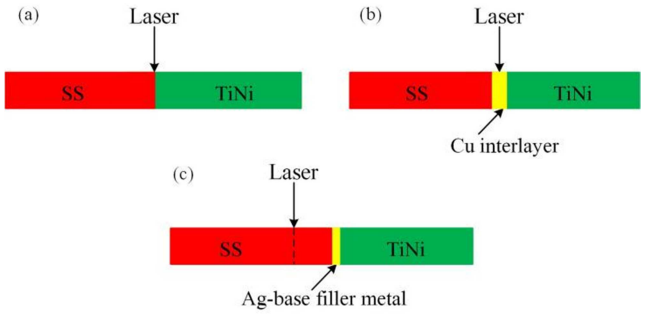

Figure 1. *Schematic diagram of the welding process: (a) joint A; (b) joint B; (c) joint C.*

2.3. Characterization Methods

The cross sections of joints were polished and etched in the reagent with 2 ml concentrated HNO_3 and 6 ml concentrated HF. The microstructure of joints were studied by optical microscopy, scanning electron microscope SEM with fast energy dispersion spectrum EDS analyzerand, and selected area XRD analysis. Microhardness tests for the weld carried out with a 10s load time and a 200g load. Tensile strength of the joints was measured by using universal testing machine with cross head speed of 2mm/min.

3. Results and Discussion

3.1. Characterization of Joint A

3.1.1. Macro-characteristics

Figure 2 shows the optical microscopy image of the cross section of joint A. It can be seen from Figure 2 that the microstructure distribution in the joint A was relatively uniform, and can be seen obvious longitudinal cracks in the joint A. The crack was located on the SS side, and cracks occur with the sound of brittle fracture after welding, the TiNi alloy/SS dissimilar materials can not be achieved the effective connection. The test results show that the average width of the joint A was about 0.83 mm, and there are no defects such as incomplete fusion, incomplete penetration, and stomatal, but obvious through cracks can be seen from the top to the bottom of the weld. The above research results show that the weldability of TiNi alloy/SS dissimilar materials was extremely poor. The main weldability problem of TiNi alloy/SS was welding cracks, which seriously deteriorates the mechanical properties of TiNi alloy/SS laser welded joints.

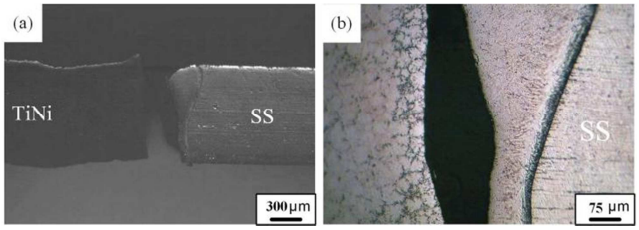

Figure 2. *Macro characteristics of joint A by laser welding without filler metal: (a) cross section; (b) fracture location.*

As is known, the occurrence of welding cracks was mainly related to the microstructure of the weld and the stress state of the joint. The chemical composition of the weld was an important factor affecting the microstructure. For the welding of TiNi alloy/SS dissimilar materials, the laser beam was focused at the TiNi alloy/SS interface under the test conditions.

The weld metal in joint A was composed of molten TiNi alloy and SS. Therefore, the chemical composition of the weld mainly depends on the fusion ratio of TiNi alloy and SS in joint A. The results show that the fusion ratios of TiNi alloy and SS are 53% and 47%, respectively. The fusion ratio of TiNi alloy (53%) was higher than that of SS (47%) mainly due to the difference of their physical properties. As the thermal conductivity of TiNi alloy (10 $Wm^{-1}.K^{-1}$) is clearly lower than thermal conductivity of SS (16.3 $Wm^{-1}.K^{-1}$), the asymmetric temperature field of joint A was formed in the welding process, which results in the high temperature zone and melting amount of TiNi alloy side was larger than that of SS side, so the fusion ratio of TiNi alloy in the joint A was larger than that of SS.

According to the references [27], the average chemical composition of weld metal welded with dissimilar materials can be calculated by formula (1):

$$C_W = D_A C_A + D_B C_B + (1 - D_{A+B})\, C_F \quad (1)$$

In the formula: C_W is the average mass fraction (%) of an alloy element in the weld metal; D_A is the dilution rate (expressed in decimal) caused by base metal A; D_B is the dilution rate (expressed in decimal) caused by base metal B; D_{A+B} is the total dilution rate (expressed in decimal) caused by base metal A and B; C_A is the mass fraction (%) of an alloy element in base metal A; C_B is the mass fraction (%) of an alloy element in base metal B; C_F is the mass fraction (%) of an alloy element in the deposited metal F. Since no filling material is added in this test, formula (1) can be simplified to formula (2):

$$C_W = D_A C_A + D_B C_B \quad (2)$$

In the formula: C_W is the average mass fraction (%) of an alloy element in the weld metal; D_A is the dilution rate caused by the TiNi alloy base metal; C_A is the mass fraction (%) of an alloy element in the TiNi alloy base metal; D_B is the dilution rate caused by the SS base metal; C_B is the mass fraction (%) of an alloy element in the SS base metal. Table 4 shows the average mass fraction of main elements in the joint A calculated by formula 1.2. The average mass fraction of the main elements (Ti, Ni, Fe) in the joint A was 23.9 wt.% Ti, 29.2 wt.% Ni, 25.3 wt.% Fe.

Table 4. *Average mass fraction of main elements in joint A (wt.%).*

Elements	Ti	Ni	Cr	Fe
Average mass fraction	23.9	29.2	8.4	25.3

3.1.2. Microstructure Analysis

The optical microscopy image of joint A is shown in Figure 3a and Figure 3b. It does not present such defects as pores and macro-cracks. SEM image of WZ_1 shown in Figure 3c indicated that joint A had a granular microstructure. Based on the analysis results in Table 4 and Ti-Fe-Ni ternary phase diagram, the main microstructure of this joint A was TiNi + $TiFe_2$. According to the microstructure analysis results of joint A, the weld was mainly composed of brittle and hard Ti-Fe and Ti-Ni intermetallics, the joint A was easy to fracture in the weld under the action of welding stress. Figure 3d shows the fracture morphology of joint A. The fracture surface has obvious brittle fracture characteristics, which shows that the macro plastic deformation of joint A was very small in the fracture process. Based on the results of the previous analysis, the joint broke along the SS side immediately after welding. A large number of Ti-Fe intermetallics are formed in the joint A, which was the root cause embrittlement of weld. On the other hand, the linear expansion coefficient of SS was significantly higher than TiNi alloy. After the laser beam passes through, the shrinkage degree of SS is larger than that of TiNi alloy in the cooling process. Because the two materials are connected together, this will lead to greater welding stress in the joint. It can be concluded that brittle Ti-Fe intermetallics are easy to form in the weld zone when laser welding of TiNi alloy and SS, and then crack under the action of welding stress.

Based on the above research results, the weldability of TiNi alloy and SS was poor, and the main weldability problem of TiNi alloy and SS was welding crack, which seriously worsens the mechanical properties of TiNi alloy/SS joint. This is mainly due to the embrittlement of weld metal and the formation of large welding stress in the joint. Due to the metallurgical reaction between Ti and Fe, a large amount of Ti-Fe intermetallic compounds are easily formed in the weld after welding. Because the brittleness of Ti-Fe intermetallics was bigger to make it embrittlement of weld metal. In addition, due to the large difference between the linear expansion coefficient of TiNi alloy and SS, a large welding stress was formed in the joint. Under the action of welding stress, the cracks are easy to initiate and extend in the embrittlement weld, which seriously worsens the mechanical properties of TiNi alloy/SS joint.

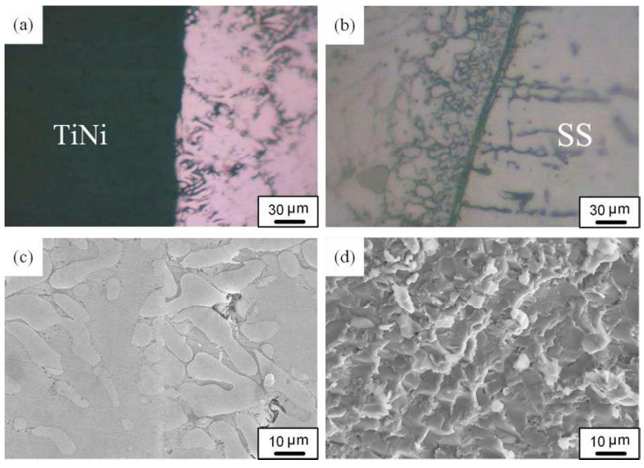

Figure 3. *Microstructures of joint A: (a) optical image of fusion line at TiNi alloy side; (b) optical image of fusion line at SS side; (c) SEM image of weld center; (d) SEM image of fracture surface.*

3.2. Characterization of Joint B

According to the previous analysis, due to the formation of a large number of brittle Ti-Fe intermetallics in the weld, the weld is prone to cause crack under the action of welding stress, which can not realize the effective connection between TiNi alloy and SS. As is known, filler material is an important

factor affecting the fusion ratio of base metal, chemical composition of weld, microstructure and mechanical properties of joint. The effect rule of pure Cu interlayer on the microstructure and mechanical properties of TiNi alloy/SS joint was studied.

3.2.1. Macro-characteristics

Figure 4 shows the optical microscopy image of the cross section of joint B. When using Cu as an interlayer, integrated joints with no obvious cracks in the weld was obtained. This means that the Cu interlayer added during welding can improve the metallurgical conditions and thus can be hopeful to improve the mechanical properties of the joints. Compared with the joint A without interlayer in section 3.1, the tendency of welding crack is obviously reduced after adding Cu interlayer, which realizes the connection of TiNi alloy/SS dissimilar materials. When welding, the melted Cu interlayer and the partially melted TiNi alloy and SS mix with each other to form a welding pool. The results of weld inspection show that the average width of the joint B is about 1.16 mm, and there are no cracks, blowhole, incomplete penetration and other defects in the joint B. The test results of joint B show that the fusion ratios of TiNi alloy and SS were 29% and 26%, respectively. Calculate the average mass fraction of main elements in the joint B according to formula (1), and the calculation results are shown in Table 5. It can be seen from Table 5 that the average contents of Ti, Fe, Cu and Ni in the joint B are 13.1 wt.% Ti, 19.5 wt.% Fe, 45 wt.% Cu and 18.3 wt.% Ni. This shows that the content of Cu in the joint B was the highest, and the content of Ti and Fe was obviously lower than that of Cu. Compared with the main components (23.9 wt.% Ti, 29.2 wt.% Ni, 25.3 wt.% Fe) of the joint A without interlayer in Section 3.1, the content of Cu element in the joint B increased significantly, while the content of Ti and Fe element decreased significantly. This is mainly due to the addition of Cu interlayer in the welding process, which reduces the melting amount of TiNi alloy and SS in the welding pool, thus reducing the content of Ti and Fe elements in the weld, thereby reducing the content of Ti-Fe intermetallics in the weld. The above changes of the chemical composition of the TiNi alloy/SS joint will affect the microstructure and the mechanical properties of the joint.

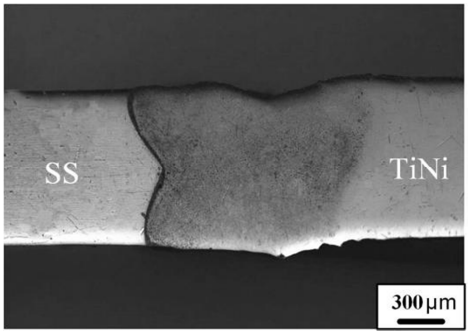

Figure 4. *Cross sections of joint B by laser welding added Cu interlayer.*

3.2.2. Microstructure Analysis

The optical microscopy image of joint B is shown in Figure 5a-c and some micro-cracks were found in it. SEM image of joint B is shown in Figure 5d. Furthermore, it can be seen from Figure 5d that microstructure of joint B presented massive and granular grains. Based on the analysis results in Table 5 and Ti-Cu-Fe ternary phase diagram, the main microstructure of this joint B was TiFe + $TiCu_2$. The Cu interlayer between TiNi alloy and SS to reduce the formation of brittle Ti-Fe intermetallics that changes character of the interaction in the melted zone and leads to formation other Ti-Cu phases than Ti-Fe-rich intermetallics. According to Fe-Cu, Cr-Cu and Ni-Cu binary alloy phase diagrams, the intermetallics do not form between Cu and Fe, Cr, Ni, although Cu-Ti intermetallics can be formed according to Ti-Cu binary alloy phase diagram, it is reported that the Ti-Cu intermetallics are not very brittle [28]. These Ti-Cu phases were found to be less brittle than the Ti-Fe intermetallics. Therefore, Cu was used as interlayer for joining TiNi alloy and SS due to the compensation of brittle Ti-Fe intermetallics by its ductility.

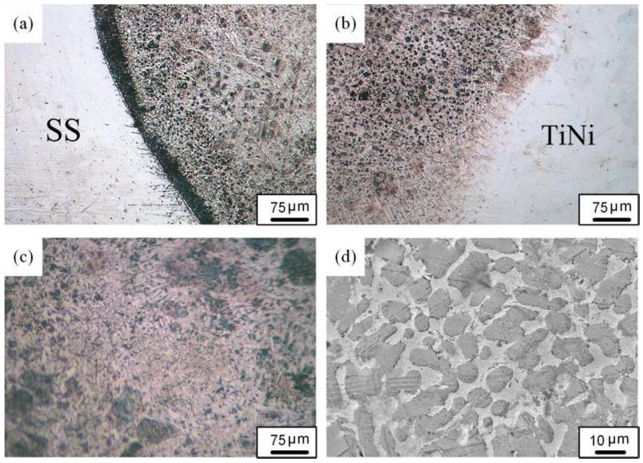

Figure 5. *Microstructures of joint B: (a) optical image of fusion line at SS side; (b) optical image of fusion line at TiNi alloy side; (c) optical image of weld center; (d) SEM image of weld center.*

Table 5. *Average mass fraction of main elements in joint B (wt.%).*

Elements	Ti	Ni	Cu	Cr	Fe
Average mass fraction	13.1	18.3	45	4.7	19.5

3.2.3. Microhardness Tests

As shown in Figure 6, the microhardness distribution in the joint B was non-uniform. The hardness of TiNi alloy was slightly lower than those of SS. But overall, the microhardness distribution in the weld metal was relatively uniform and average microhardness in the weld metal was 522 HV which was higher than that of SS. This was mainly resulted from Ti-Fe and Ti-Cu intermetallics. Moreover, hardness variation also corroborates the microstructural investigation regarding the extent of Cu mixing in the weld metal. Hardness distribution further reveals that Cu was uniformly dispersed in the weld metal. Therefore it can relatively deform easily to reduce the residual stresses in the inner of joint B. Although these Ti-Cu intermetallics were hard, they had relatively lower hardness compared with Ti-Fe intermetallics.

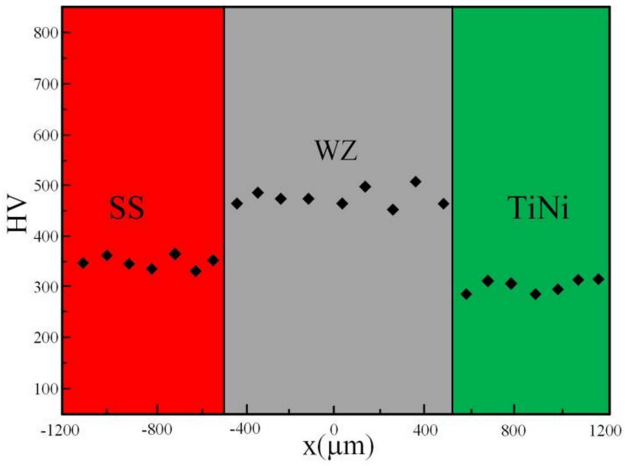

Figure 6. *Vickers microhardness measurements at semi-height of joint B (zero point situated in the center of joint B).*

3.2.4. Tensile Tests and Fracture Analysis

The maximum tensile strength of the joint was 198 MPa (Figure 7a). As shown in Figure 7b, fracture occurred in the weld middle at joint B. SEM image of the fracture surfaces were presented in Figure 7c, fracture surfaces were characterized by a number of secondary crack zone. That means the fracture mode of the joint was brittle fracture. As shown in Figure 7d, XRD analysis of fracture surface detected TiFe and $TiCu_2$ phases. This confirmed the presence of a large number of Ti-Cu and Ti-Fe intermetallics at fracture surfaces.

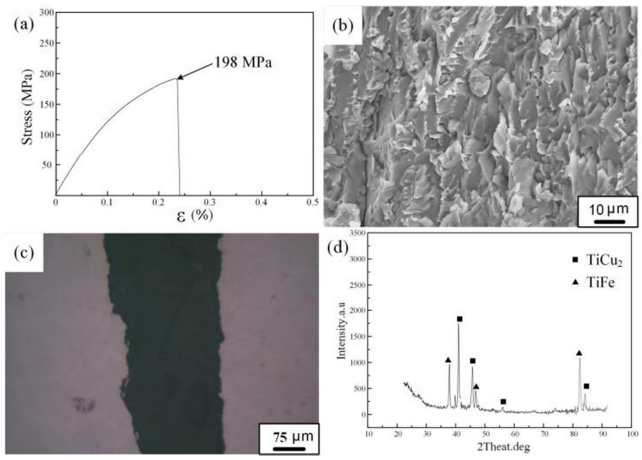

Figure 7. *Tensile test results of joint B: (a) tensile test curve; (b) fracture location; (c) SEM image of fracture surface; (d) XRD analysis results of fracture surface.*

Based on the above research results, the laser welded joints basically achieve the effective connection between TiNi alloy and SS after adding Cu interlayer. Because the addition of Cu interlayer reduces the melting amount of base metal on both sides and inhibits the liquid mixing of TiNi alloy and SS during welding, it reduces the content of Ti-Fe intermetallics in the weld and makes its discontinuous distribution in the weld. However, as long as the Cu interlayer melts completely in the weld, Ti and Fe elements will mix and react in the molten pool, and Ti-Fe intermetallic compounds will inevitably form in the weld. That is to say, the formation of Ti-Fe intermetallic compounds in the weld can be inhibited by adding interlayer, but it can not be completely eliminated. The existence of Ti-Fe intermetallics still has a great influence on the properties of the joint. Therefore, the formation of Ti-Fe intermetallics cannot be avoided only by adding an interlayer. If we want to further improve the performance of the joint, we need to optimize the welding structure to avoid the formation of Ti-Fe intermetallics.

3.3. Characterization of Joint C

According to the previous research results, the microstructure and mechanical properties of TiNi alloy/SS joint can be improved by adding appropriate interlayer materials, but the formation of brittle and hard Ti-Fe intermetallic compounds in the weld can not be avoided. In order to further improve the mechanical properties of TiNi alloy/SS joint, the design idea of laser welding of TiNi alloy and SS assisted by metal transition layer is proposed in this paper. The purpose is to avoid the metallurgical reaction between Ti and Fe, with improve the microstructure and mechanical properties of TiNi alloy/SS joint.

3.3.1. Macro-characteristics

The optical microscopy image of the cross section of the joint C is shown in Figure 8a. The joint C can fall into three parts: the fusion weld formed at the SS side, unmelted SS and the brazed weld formed at the TiNi-SS interface. The fusion weld did not form Ti-Fe intermetallics due to the presence of unmelted SS. The average width of fusion weld, unmelted SS and brazed weld was 1.4 mm, 0.21 mm and 0.14 mm, respectively. Because the microstructure of the fusion weld is quite different from that of the brazed weld, the brazed weld becomes black after corrosion. Figure 8b presents the optical image before corrosion of the brazed weld. It does not present such defects as pores and macro-cracks. The unmelted part of SS acted as a heat sink absorbing a significant amount of energy from the welding pool and transferring it to the TiNi alloy side [29-30]. Hence, the filler metal of TiNi-SS interface had a high temperature during welding although it was not subjected to laser radiation. The temperature was high enough to promote filler metal melting. This meets the temperature requirement for brazed welding. Moreover, the local heating of the SS side caused uneven volume expansion and thermal stress was produced, which helped to obtain an intimate contact between the TiNi alloy, Ag-based fillers and SS surface. The high temperature and the intimate contact at the TiNi-SS interface provided favorable conditions for atomic interdiffusion, which subsequently led to brazing process at the TiNi-SS interface. Compared with the joint A without interlayer and joint B added Cu interlayer in section 3.1 and 3.2, the unmelted SS acted as a barrier to mixing of the two base materials, which eliminated the formation of brittle Ti-Fe intermetallics in the joint C. Additionally, the unmelted SS was beneficial to relieve and accommodate the thermal stress in the joint C, which could help to improve the mechanical properties of the joints.

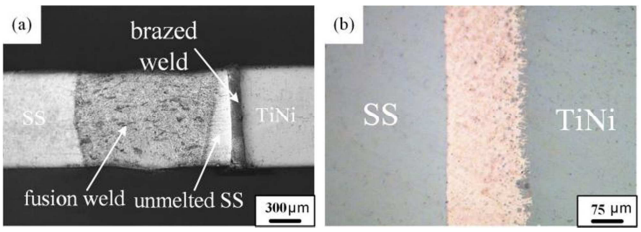

Figure 8. *Macroscopic feature of the joint C: (a) optical image of the cross section of the joint C; (b) optical image before corrosion of the SS-TiNi alloy interface.*

3.3.2. Microstructure Analysis

The optical image of the fusion weld is shown in Figure 9a, and no defects were observed in it. SEM image of the fusion weld is shown in Figure 9b. The fusion weld mainly consists of acicular structure. The optical image of the brazed weld at TiNi-SS interface is shown in Figure 9c. It can be observed that, the brazed weld contained three zones marked as I, II and III sorted by their morphologies and colors. Figure 9d, Figure 9e and Figure 9f correspond to the three zones in Figure 9c, respectively. The compositions of each zone (denoted by letter A-C in Figure 9) were studied using SEM-EDS. EDS analysis was applied to these zones to measure the compositions of the reaction products and the results are listed in Table 6. Based on the previous analysis, the microstructure of the brazed weld was mainly composed of Ag-based fillers. The chemical composition of zone I was consistent with the Ag-based fillers. Based on the EDS analyses results and Ag-Cu-Zn phase diagram, the main microstructure of zone I was defined as $AgZn_3$ + CuZn phase. When the laser beam was focused on one side of the SS, elemental diffusion between the matrix material and the filler metal occurred immediately, resulting into their composition to deviate from the original composition. Therefore, liquid phase formation and elemental diffusion occurred simultaneously. At this moment, the dissolution of Ti and Fe into the filler metal occurred under the high concentration gradient, which formed solid-phase reaction layer, and this reaction layer exists only in the smaller region of the TiNi-SS interface. As shown in Figure 9e and 9f, zone II and zone III were reaction layers formed by element diffusion. Based on Fe-Cu-Zn phase diagram, the microstructure of zone II was defined as Fe_3Zn_2 + CuZn. Based on Cu-Ti-Zn phase diagram, the microstructure of zone III was defined as Cu_2Ti + Ti_2Zn_3. Therefore, the main microstructures of diffusion weld were Fe_3Zn_2 + CuZn, $AgZn_3$ + CuZn and Cu_2Ti + Ti_2Zn_3.

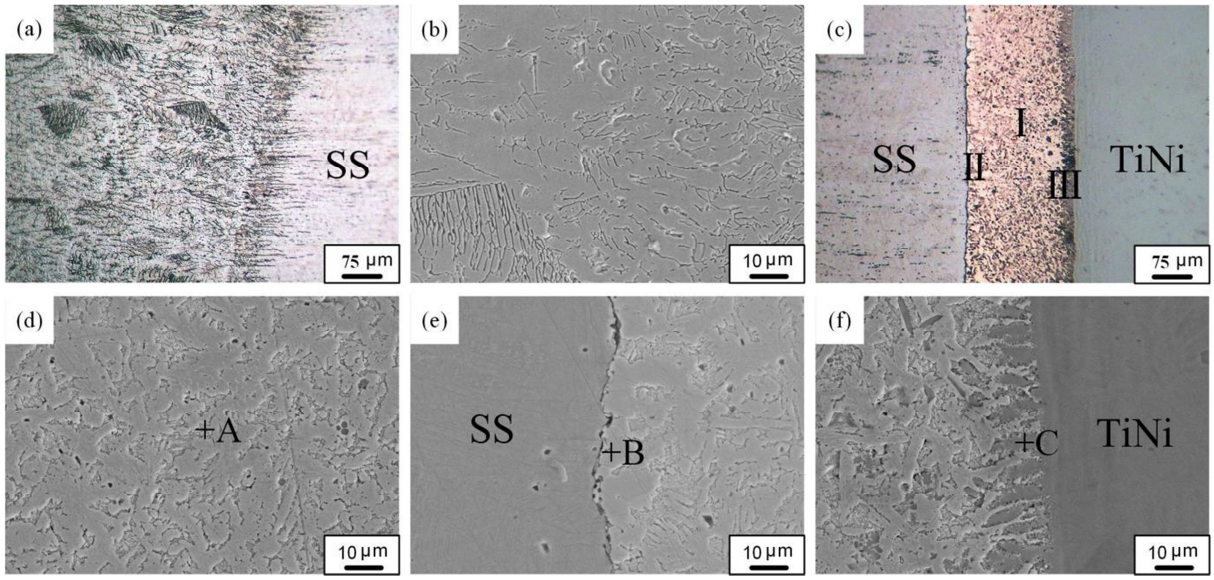

Figure 9. *Microstructures of the joint C： (a) optical image of fusion zone; (b) SEM image of fusion zone; (c) optical image of the brazed weld; (b) SEM image of the zone I in Figure 9c; (c) SEM image of the zone II in Figure 9c; (d) SEM image of the zone III in Figure 9c.*

Table 6. *The chemical composition of each phase in joint C (wt.%).*

Region	Composition%							Potential phases
	Ti	Ag	Fe	Cu	Zn	Cr	Ni	
A			29.1	23.5	46.6			$AgZn_3$ + CuZn
B		15.4	46.4	21.2	11.3			Fe_3Zn_2 + CuZn
C	19.6		34.4	26.2	8.4		12.1	Cu_2Ti + Ti_2Zn_3

3.3.3. Microhardness Tests

As shown in Figure 10, the microhardness distribution in the joint C was non-uniform. It can be seen from Figure 10 that the microhardness distribution in the fusion weld was not-uniform, approximately W type. The microhardness of the fusion weld was significantly reduced compared to the 304 SS. The hardness of the brazed weld was very low compared to the fusion weld. The hardness of brazed weld was low because filler metal was simple metals. Therefore it can relatively deform easily to reduce the residual stresses in the inner of TiNi-SS joint.

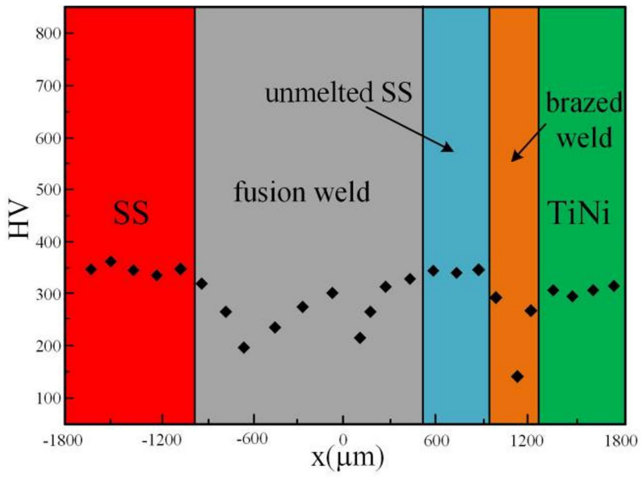

Figure 10. *Vickers microhardness measurements at semi-height of joint C (zero point situated in the center of joint C).*

3.3.4. Tensile Tests and Fracture Analysis

The maximum tensile strength of the joint was about 225 MPa (Figure 11a). The joint fractured in SS side of the brazed weld during tensile tests (Figure 11b). Figure 11c shows fracture surface of the joint exhibiting typical brittle characteristics. Moreover, as shown in Figure 11d, XRD analyses of fracture surface detected Fe_3Zn_2 and CuZn phases. This confirmed the presence of Fe-Zn and Cu-Zn intermetallics at fracture surfaces. It should be noted that there was no Ti-Fe intermetallics in the brazed weld. Reaction layer at SS side in brazed weld became the weak zone of the joint, which led to the failure in the tensile test.

Based on the above results, the formation of Ti-Fe intermetallic compounds is avoided due to the presence of unmelted SS in the joint. Only a small amount of Ti-Cu and Fe-Zn intermetallics is formed in the reaction layer at the TiNi-SS interface. Due to the rapid heating and cooling speed of laser welding, the holding time at high temperature is short, and it is easy to form a narrow reaction zone at the TiNi-SS interface. In addition, higher cooling rate inhibited the growth of dendrite structure in the reaction zone. Therefore, it is easy to obtain fine microstructure in the reaction zone, which is conducive to reducing the brittleness of the reaction layer. The results show that the formation of narrow reaction layer and fine metallurgical structure at the interface is one of the main reasons to improve the joint strength.

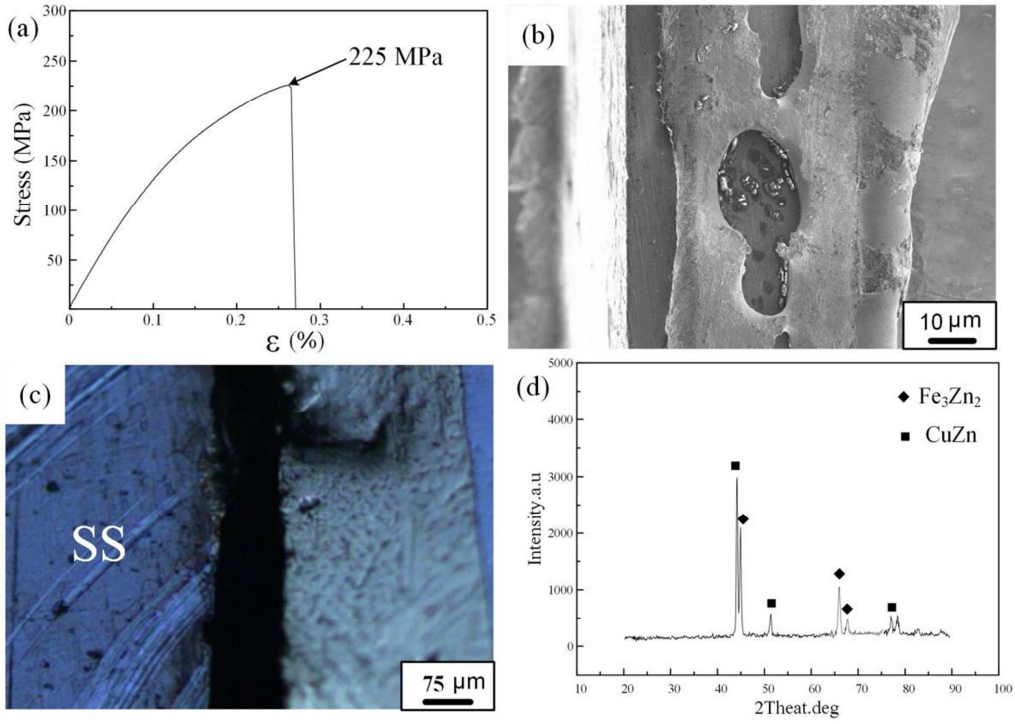

Figure 11. *Tensile test results of joint C: (a) tensile test curve; (b) fracture location; (c) SEM image of fracture surface; (d) XRD analysis results of fracture surface.*

4. Conclusions

The possibility of three welding processes for connect TiNi alloy to SS with when no interlayer, Cu sheet as interlayer and Cu-base filler metal was studied. The main conclusions are presented below.

1) For joint A with laser offset of zero, when TiNi alloy is mixed with the SS in the liquid state, a number of brittle Ti-Fe intermetallics are formed inside weld zone during welding. The direct fusion welding of these two kinds of base materials leads to the continuous distribution of Ti-Fe intermetallics in the weld zone, resulting in very great brittleness in the joint A until the fractured.
2) For joint B with laser offset of zero, the amount of Ti-Fe intermetallics in the weld reduced by using Cu as interlayer during laser welding of TiNi alloy to SS and their distribution were discontinuous. It can reduce the

brittleness of Ti-Fe intermetallics, and thus can be to improve the mechanical properties of the joints. The tensile strengths of the joints were dependent on microstructure, which is about 198 MPa.

3) For joint C with a laser beam offset of 1.0 mm for SS, the unmelted SS was selected as an barrier to avoid mixing of the TiNi alloy and SS which eliminated the formation of brittle Ti-Fe intermetallics in the joint C. A brazed weld was formed at the TiNi alloy-SS interface with the main microstructure of Fe_3Zn_2 + CuZn, $AgZn_3$ + CuZn and Cu_2Ti + Ti_2Zn_3. A great amount of atomic diffusion occurs at the TiNi alloy-SS interface during welding, and the thickness of brazed weld can reach hundreds of micrometres. The tensile resistance of the joint was determined by brazed weld. The maximum tensile strength of joint was 225 MPa.

Conflict of Interest

All the authors do not have any possible conflicts of interest.

References

[1] Patoor E, Lagoudas DC, Entchev PB, Brinson LC, Gao XJ. Shape memory alloys. Part I: general properties and modeling of single crystals. *Mech Mater.* 38 (2006), 391-429.

[2] Yang DZ. Shape memory alloy and smart hybrid composites-advanced materials for the 21st century. *Mater Des.* 21 (6) (2000), 503-5.

[3] Predki W, Knopik A, Bauer B. Engineering applications of TiNi shape memory alloys. *Mater Sci Eng A*. 481-482 (2008), 598-601.

[4] Wang ZG, Zu XT, Feng XD, Zhu S, Bao JW, Wang LM. Characteristics of two-way shape memory TiNi springs driven by electrical current. *Mater Des.* 25 (8) (2004), 699-703.

[5] Falvo A, Furgiuele FM, Maletta C. Laser welding of a TiNi alloy: mechanical and shape memory behaviour. *Mater Sci Eng A*. 412 (2005), 235-40.

[6] Yan Z, Daqian S, Xiaoyan G, et al. Nd/YAG pulsed laser welding of TC4 titanium alloy to 301L stainless steel via pure copper interlayer. *international journal of advanced manufacturing technology* 90 (1-4) (2017), 953-961.

[7] Yan Z, Daqian S, Xiaoyan G, et al. A hybrid joint based on two kinds of bonding mechanisms for Titanium alloy and stainless steel by pulsed laser welding. *Materials Letters* 185 (2016), 152-155.

[8] Yan Z, Daqian S, Xiaoyan G, et al. Microstructure and mechanical property improvement of dissimilar metal joints for TC4 Ti alloy to 301L stainless steel. *journal of materials science* 53 (4) (2018), 2942-2955.

[9] Yan Z, Daqian S, Xiaoyan G, et al. Nd/YAG pulsed laser welding of TC4 Ti alloy to 301L stainless steel using Ta/V/Fe composite interlayer. *Materials Letters* 212 (2018), 54-57.

[10] Oliveira JP, Panton B, Zengb Z, Andrei CM, Zhou Y, Miranda RM, et al. *Acta Mater* 105 (2016), 10-5.

[11] Li HM, Sun DQ, Han YW, Dong P, Liu C. Microstructures and mechanical properties of laser-welded TiNi shape memory alloy and stainless steel wires. *China Weld* 19 (3) (2010), 1-5.

[12] Yan Z, Daqian S, Xiaoyan G, et al. Nd YAG pulsed laser welding of dissimilar metals of titanium alloy to stainless steel. *international journal of advanced manufacturing technology* 94 (1-4) (2018), 1073-1085.

[13] Song YG, Li WS, Li L, Zheng YF. The influence of laser welding parameters on the microstructure and mechanical property of the as-jointed TiNi alloy wires. *Mater Lett* 62 (2008), 2325-8.

[14] Yan Z, Daqian S, Xiaoyan G, et al. Strength improvement and interface characteristic of direct laser welded Ti alloy/stainless steel joint. *Materials Letters* 231 (2018), 31-34.

[15] Yan Z, Daqian S, Xiaoyan G, et al. Microstructure and mechanical property improvement of laser welded TC4 Titanium alloy and 301L stainless steel joints without filler metal. *Journal of Materials Engineering and Performance*. 28 (1) (2019), 140-153.

[16] Borrisutthekul R, Yachi T, Miyashita Y, Mutoh Y. *Mater Sci Eng A*. 467 (2007), 108-13.

[17] H. M. Li, D. Q. Sun,, X. L. Cai, P. Dong, W. Q. Wang. Laser welding of TiNi shape memory alloy and stainless steel using Ni interlayer. *Materials and Design*. 39 (2012), 285-293.

[18] Bricknell RH, Melton KN, Mercier O. The structure of TiNiCu shape memory alloys. *Metall Trans A.* 10 (1979), 693-7.

[19] A. Shojaei Zoerama, A. Rahmani, S. A. A. Akbari Mousavi. Microstructure and properties analysis of laser-welded Ni–Ti and 316l sheets using copper interlayer. *Journal of Manufacturing Processes*. 26 (2017), 355-363.

[20] Yan Z, Daqian S, Xiaoyan G, et al. Characterization of laser-welded Ti alloy and stainless steel joint using Cu interlayer. *Journal of Materials Engineering and Performance.* 28 (2019), 6092-6101.

[21] Yan Z, Yankun C, Jianping Z, et al. Experimental and numerical study on microstructure and mechanical properties for laser welding-brazing of TC4 Titanium alloy and 304 stainless steel with Cu-base filler metal. *Journal of Materials Research and Technology*. 9 (1) (2020), 465-477.

[22] Wang YL, Li H, Li ZX, Feng JC. Research on transient liquid phase diffusion bonding process of TiNi shape memory alloy to stainless steel. *J Mater Eng* 2008: 48-51. [in Chinese].

[23] Li H, Li ZX, Wang YL, Feng JC. Transient liquid phase diffusion bonding of TiNi shape memory alloy and stainless steel. *Rare Metal Mater Eng.* 40 (8) (2011), 1382-6 [in Chinese].

[24] Qiu XM, Li MG, Sun DQ, Liu WH. Study on brazing of TiNi shape memory alloy with stainless steels. *J Mater Process Technol*. 176 (2006), 8-12.

[25] Seki M, Yamamoto H, Nojiri M, Uenishi K, Kobayashi KF. Brazing of Ti–Ni shape memory alloy with stainless steel. *J Jpn Inst Metals.* 64 (2000), 632-40.

[26] Fukumoto S, Inoue T, Mizuno S, Okita K, Tomita T, Yamamoto A. Friction welding of TiNi alloy to stainless steel using Ni interlayer. *Sci Tech Weld Join.* 15 (2) (2010), 124-30.

[27] Wei Li, Lei Yan, Sreekar Karnati. Ti-Fe intermetallics analysis and control in joining titanium alloy and stainless steel by Laser Metal Deposition. *Journal of Materials Processing Technology* 242 (2017), 39-48.

[28] Zhao DS, Yan JC, Wang CW, Wang Y, Yang SQ. Interfacial structure and mechanical properties of hot rool bonded joints between titanium alloy and stainless steel using copper interlayer. *Sci Technol Weld Join*. 13 (2008), 765-8.

[29] Yan Z, Yuanbo B, Jianping Z, DaQian S, HongMei L. Strength improvement and interface characteristic of TC4 Ti alloy and 304 stainless steel joint based on a hybrid connection mechanism. *Journal of Materials Research and Technology*. 9 (2) (2020), 1340-1343.

[30] Yan Z, Yidi G, Jianping Z, et al. Butt laser welding of TC4 Titanium alloy and 304 stainless steel with Ag-base filler metal based on a hybrid connection mechanism. *Optics and Laser Technology*. 124 (2019), 105957.